Structural Engineering and Mechanics, *Vol. 57, No. 2 (2016) 265-280*
DOI: http://dx.doi.org/10.12989/sem.2016.57.2.265

Prediction of residual mechanical behavior of heat-exposed LWAC short column: a NLFE model

Yasmeen T. Obaidat*[1] and Rami H. Haddad[2a]

[1]*Civil Engineering Department, Yarmouk University, P.O. Box 566, Irbid, Jordan*
[2]*Civil Engineering Department, Jordan University of Science and Technology, P.O. Box 22110, 22110 Irbid, Jordan*

(Received February 15, 2015, Revised November 30, 2015, Accepted December 14, 2015)

Abstract. A NLFE model was proposed to investigate the mechanical behavior of short columns, cast using plain or fibrous lightweight aggregate concrete (LWAC), and subjected to elevated temperatures of up to 700°C. The model was validated, before its predictions were extended to study the effect of other variables, not studied experimentally. The three-dimensional NLFE model was developed using ANSYS software and involved rational simulation of thermal mechanical behavior of plain and fibrous LWAC as well as longitudinal and lateral steel reinforcement. The prediction from the NLFE model of columns' mechanical behavior, as represented by the stress-strain diagram and its characteristics, compared well with the experimental results. The predictions of the proposed models, considering wide range of lateral reinforcement ratios, confirmed the behaviors observed experimentally and stipulated the importance of steel confinement in preserving post-heating mechanical properties of plain and fibrous LWAC columns, being subjected to high temperature.

Keywords: NLFE; fire; post-heating; mechanical properties; columns; lightweight concrete

1. Introduction

One of the several causes of failure of reinforced concrete structures is the exposure to an accidental fire. Relevant research works have attempted to establish an understanding for the behavior of concrete materials and structural integrity upon exposure to elevated temperature (Arioz 2007, Lawson *et al.* 2000, Issa *et al.* 2004, Haddad *et al.* 2008). The outcome indicated that the mechanical properties would be detrimentally affected by elevated temperature; represented in loss of strength and elasticity modulus and an increase in ductility with possible spalling in structural elements of relatively large size and/or cast using high strength concrete. RC columns are the main load bearing elements in concrete structures as they support beams and slabs and convey live and dead loads to foundations. Therefore, their weakening or failure under an accidental fire results in catastrophic consequences represented in partial to entire collapse of fire-exposed concrete facilitates. In fact, the most present findings revealed that concrete columns may

*Corresponding author, Assistant Professor, E-mail: yasmin.o@yu.edu.jo
[a]Professor

http://www.techno-press.org/?journal=sem&subpage=8 ISSN: 1225-4568 (Print), 1598-6217 (Online)

loss up to 50% of their load bearing capacity when heated to 500℃, before showing a dramatic reduction at temperatures in excess of 700℃ (Haddad and Ashour 2013, Al-Nimry *et al.* 2014). Exposure of columns to elevated temperatures would also reduce the elastic modulus of confined concrete as well as the yield strength of reinforcing steel.

Nowadays, there is an increasing trend towards the utilization of lightweight aggregate concrete (LWAC) in construction industry; especially green house systems, because of the many advantages it possesses over conventional concrete of same strength grade; represented in lower dead load, improved heat and sound insulation, and better resistance to dynamics load, (Demirbog and Gu 2003, Kayali 2008, Mouli and khelafi 2008, Hossain *et al*. 2006, FIP 2007). To overcome the problems associated with LWAC brittleness, steel fibers of varying geometric properties and aspect ratio are usually incorporated into LWAC to increase its ductility (Banthia and Sappakittipakorn 2007, Chen and Liu 2005).

In recent years, nonlinear finite element (NLFE) modeling has been utilized extensively in simulating the structural behavior of various RC elements; as it accounts for the nonlinear response of concrete and steel. Hence, experimental results can be validated, before the NLFE model is extended for predictions of cases, not studied experimentally. Consequently, time and cost of experiments are reduced and satisfactory amount of data generated for further statistical analysis and modeling. Many researchers have employed NLFE methods to simulate structural behaviors of concrete elements exposed to elevated temperature; following different approaches.

Nizamuddin and Bresler (1979) performed a nonlinear finite element model based on Kirchhoff thin plate theory and included the coupling of bending and membrane action for the analysis of reinforced concrete slabs under fire. On other hand, Ahmed and Hasan (2005) used finite difference method with dynamic relaxation technique to study the effect of cyclic heating and cooling on the nonlinear behaviour of reinforced concrete slabs at different load conditions before and after cracking up to failure. In another study, Huang (2010) stipulated that the bond condition between the concrete and reinforcing steel have an important impact on the fire resistance of reinforced concrete structures, especially when exposure temperature exceeds 500℃. Recently, Pothisiri and Panedpojaman (2012) modeled the bond degradation of reinforcing steel in concrete subject to elevated temperatures by taking into account tension softening behavior of concrete under high temperatures. Dwaikat *et al*. (2009) used a macroscopic finite element model for studying the influence of various parameters on fire resistance of RC beams then developed a simplified expression utilizing generated data for predicting the fire resistance of RC beams.

In the present paper, a NLFE model is proposed to simulate thermal mechanical performance of plain and fibrous LWAC concrete short columns, and validated using refereed data before its prediction are extended for parameters, not studied experimentally. The validation data used are from a published work led by the second author Haddad and Ashour (2013).

2. Nonlinear finite element modeling

2.1 Introduction

The present numerical modeling of plain and fibrous LWAC columns, pre-exposed to elevated temperatures, was performed using a 3D nonlinear finite element method using the program ANSYS, ANSYS (2008). The following sections briefly summarize the finite element modeling; including element type for each component of the column testing assembly, boundary conditions,

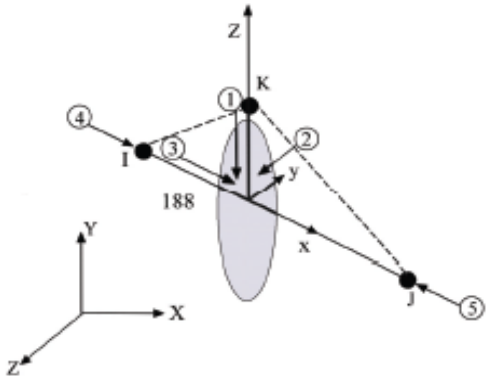

Fig. 1 Beam 188-3D linear beam, ANSYS (2008)

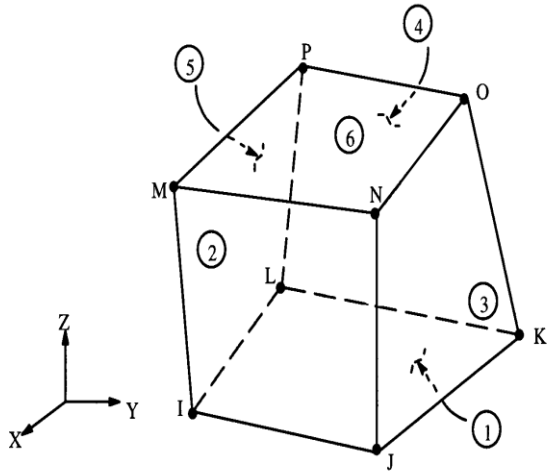

Fig. 2 Solid65, 3D solid, ANSYS (2008)

and material properties.

2.2 Element types for different components

Three different types of elements for reinforcing steel, concrete, and steel fibers were used in the present NLFE modeling.

2.2.1 Steel reinforcement

A beam element 188 was used for the steel reinforcement with configurations, shown in Fig. 1. The element has two nodes with six degrees of freedom translation in *x*, *y* and *z* directions and rotation about *x*, *y* and *z* direction.

2.2.2 Concrete

The solid 65 element was used to model the concrete. This element has eight nodes with three degree freedom of translation in *x*, *y*, and *z* directions at each node, as shown in Fig. 2. The chosen

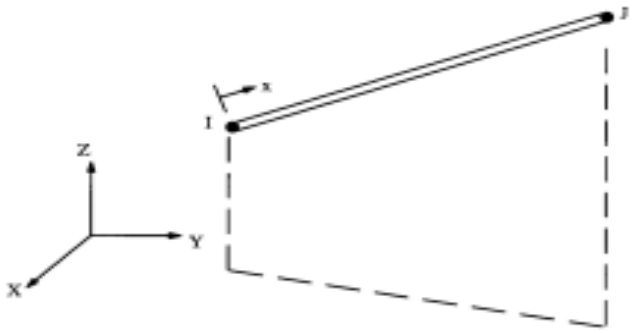

Fig. 3 Link8 -3D spar for steel fibers, ANSYS (2008)

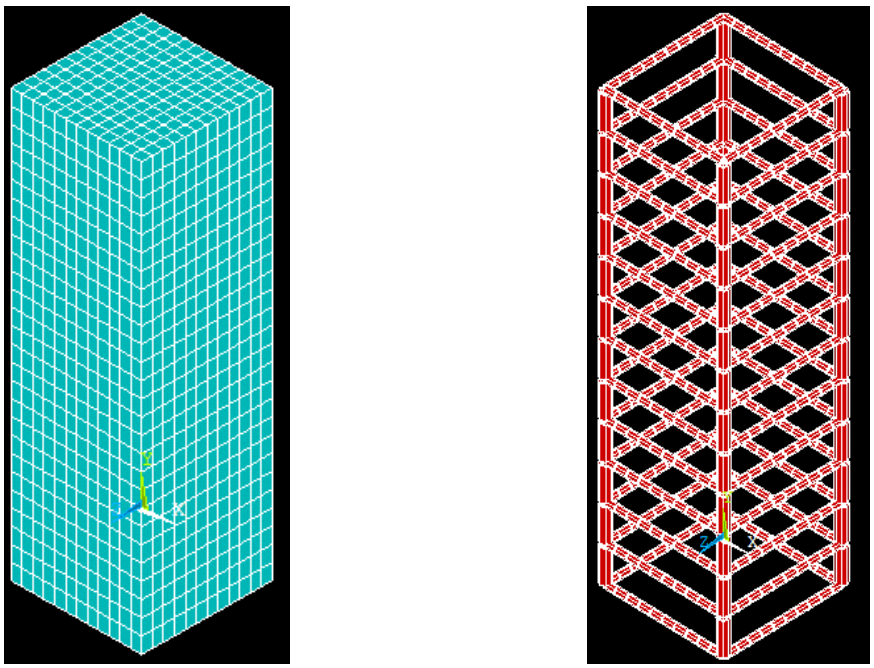

(a) Concrete (b) Steel

Fig. 4 Finite element discretization of concrete and reinforcement and boundary conditions

element is capable of cracking in tension and crushing in compression.

2.2.3 Steel fibers

Steel fibers were modeled using link 8-3D spar element, which has 2-nodes with three degrees of freedom in nodal *x*, *y* and *z* directions with its geometry shown in Fig. 3. The orientation of the fibers within an element is modeled considering different orientations of 0, 45, and 90.

2.3 Modeling load, and boundary conditions

The boundary conditions were assumed such that the top surface of all columns was translation

restricted in *x* and *z* directions and displacement allowed in *y* direction, whereas the bottom surface of the columns was simulated as displacement restricted in all directions. Newton Raphson method was used and involved an iterative procedure until providing convergent solution with displacement control conditions adopted, ANSYS (2008). The NLFE meshing of the column and reinforcement is demonstrated in Fig. 4.

2.4 Modeling of materials

2.4.1 Concrete

Concrete in compression and compression was modeled as a nonlinear isotropic material. This model is associated with Von Mises Criterion coupled with isotropic work hardening method, ANSYS (2008). The stress-strain curve for concrete in compression was assumed as linear-elastic until a stage corresponding to micro-crack initiation, after which the relationship was assumed nonlinear until ultimate stress then failure. On the other hand, the stress-strain curve for concrete in tension was assumed linear-elastic until the ultimate tensile strength, without a softening portion. The stress-strain model depicting concrete in compression is shown in Fig. 5. It is described by the following equation, Seanz (1964)

$$\sigma_c = \frac{E_c \varepsilon_c}{1 + (R + R_E - 2)(\frac{\varepsilon_c}{\varepsilon_o}) - (2R - 1)(\frac{\varepsilon_c}{\varepsilon_o})^2 + R(\frac{\varepsilon_c}{\varepsilon_o})^2} \tag{1}$$

Where:

$$\begin{cases} R = \dfrac{R_E (R_\sigma - 1)}{(R_\varepsilon - 1)^2} - \dfrac{1}{R_\varepsilon} \\ R_E = \dfrac{E_c}{E_o} \\ E_0 = \dfrac{f_c'}{\varepsilon_0} \end{cases}$$

R_ε=4; R_σ=4; as reported in the work of Hu and Schnobrich, Hu and Schnobrich (1989) ε_0 as obtained from Table 1.

The elastic modulus and tensile strength were calculated according to the ACI code (2011) and given in Eqs. (2)-(3). Poisson's ratio was assumed constant at (0.2).

$$f_{ct} = 0.6\lambda\sqrt{f_c'} \tag{2}$$

$$E_c = 4700\sqrt{f_c'} \tag{3}$$

Where, λ=0.85 for light weight concrete; and f'_c is the cylinder compressive strength for concrete (MPa).

To account for the degradation in the mechanical properties of concrete under elevated temperatures, Eqs. (4) through (6) were used to estimate values of compressive strength, strain at ultimate stress and elastic modulus, respectively, EN 1994-2. Those were used as input data for modeling the behavior of columns under high temperature.

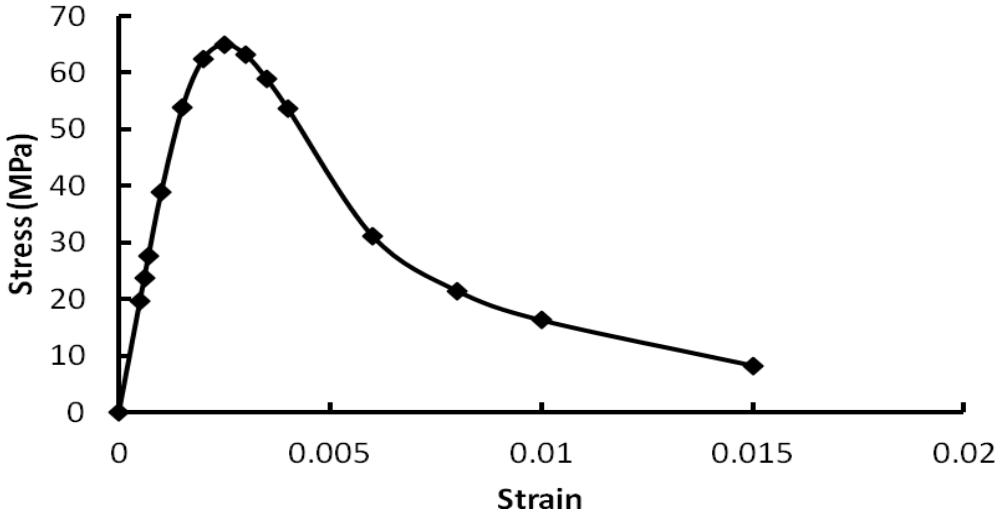

Fig. 5 Stress-strain relationship for concrete under uni-axial compression

$$f_{cr}^{'} / f_{o}^{'} = \begin{cases} 1.01 - 0.00055\,T & , \quad 20^{o}C < T \le 200^{o}C \\ 1.15 - 0.00125\,T & , \quad 200^{o}C \le T < 800^{o}C \end{cases} \tag{4}$$

$$\varepsilon_{cr} / \varepsilon_{o} = \begin{cases} 1 & , \quad 20^{o}C < T \le 200^{o}C \\ (-0.1\,f_{c}^{'} + 7.7)\left[\dfrac{\exp(-5.8 + 0.01T)}{1 + \exp(-5.8 + 0.01T)} - 0.0219\right] + 1 & , \quad 200^{o}C \le T < 800^{o}C \end{cases} \tag{5}$$

$$E_{cr} / E_{o} = -0.00165T + 1.033 \quad , \quad 20^{o}C < T \le 600^{o}C \tag{6}$$

2.4.2 Steel reinforcement and fibers

The steel reinforcement and fibers were assumed to be elastic-plastic materials with corresponding stresses calculated according to Eqs. (7) and (8).

$$f_s = E_s \varepsilon_s \,, \quad \varepsilon_s \le \varepsilon_y \tag{7}$$

$$f_s = f_y \,, \quad \varepsilon_s > \varepsilon_y \tag{8}$$

Where,

f_s and f_y: the stress and yield stress of steel (MPa), respectively; and

E_s : the elastic modulus of stress (MPa); and

ε_s and ε_y: the strain and yield strain of steel (mm/mm).

The reduction in elastic modulus and yield stress for steel due to high temperature were calculated according to Eq. (9), EN 1994-1-2

$$\frac{f_{s,T}}{f_y} = [0.967\,(1 + \exp[\frac{T - 482}{39.19}])]^{-\frac{1}{3.833}} \tag{9}$$

Table 1 Variation in mechanical properties of concrete and steel with temperature, EN 1994-1-2

Temperature (^{o}C)	Concrete		Steel	Steel Fiber
	Compressive strength (MPa)	Maximum Strain (mm/mm)	Yield stress (MPa)	Yield stress (MPa)
23	65	0.00250	590	1172
300	50	0.00274	569	1131
400	42	0.00354	554	1099
500	34	0.00558	445	885
600	26	0.00923	259	510
700	18	0.01350	134	265

Where $f_{s,T}$ and f_y: the yield strength at elevated and room temperatures, respectively, Table 1.

2.4.3 Bond between concrete and steel

Considering that the predominant stresses in the current problem is compressive, prefect bond was assumed between reinforcing steel or steel fibers and concrete until failure.

3. Validation of the NLFE model

3.1 Introduction

The results from compressive stress response on intact or thermally-damaged plain and fibrous LWAC short columns, in Haddad and Ashour (2013) were used for validating the present NLFE model. The experimental study comprised from a total of seventy two scaled plain and fibrous LWAC columns, prepared without and with moderate to high transverse reinforcement ratios, before subjected to elevated temperatures in the range from 300 to 700℃, and tested under compression. Obtained results were analyzed for major mechanical properties, compressive strength capacity, stiffness modulus, strain at ultimate stress, and compressive toughness. The LWAC columns had the geometric configuration and reinforcement detailing of Fig. 6: each column had a total length of 400 mm, and cross section of (120×120 mm^2) with four 10-mm reinforcing steel bars for longitudinal reinforcement and 6-mm-diameter steel bars for lateral reinforcement (ties). The two tie spacing studied at 30 and 60 mm corresponded to transverse steel ratios of 1.57 and 3.14%, respectively. The latter were computed using the formula: $\rho_{sv} = \frac{4 \times A_{sh}}{s_t h}$; where ρ_{sv} are transverse confinement ratio; A_{sh} is the cross- sectional area of a transverse tie ($\pi \times 6^2/4$=28.27 mm^2); s_t is the tie spacing; and h=120 mm is the cross-sectional dimension of the specimen.

A concrete cover of 20 mm was used for the top and bottom ends, whereas a concrete cover of 10 mm was used on the sides. The testing setup for all columns investigated is shown in Fig. 6. The LWAC mixtures, without and with 1% volumetric fraction of steel fibers, were designed to achieve an unconfined compressive strength of about 65 MPa using Type I cement and natural coarse and fine aggregates. The column specimens were crushed to failure under a load rate of 120 kN/minute.

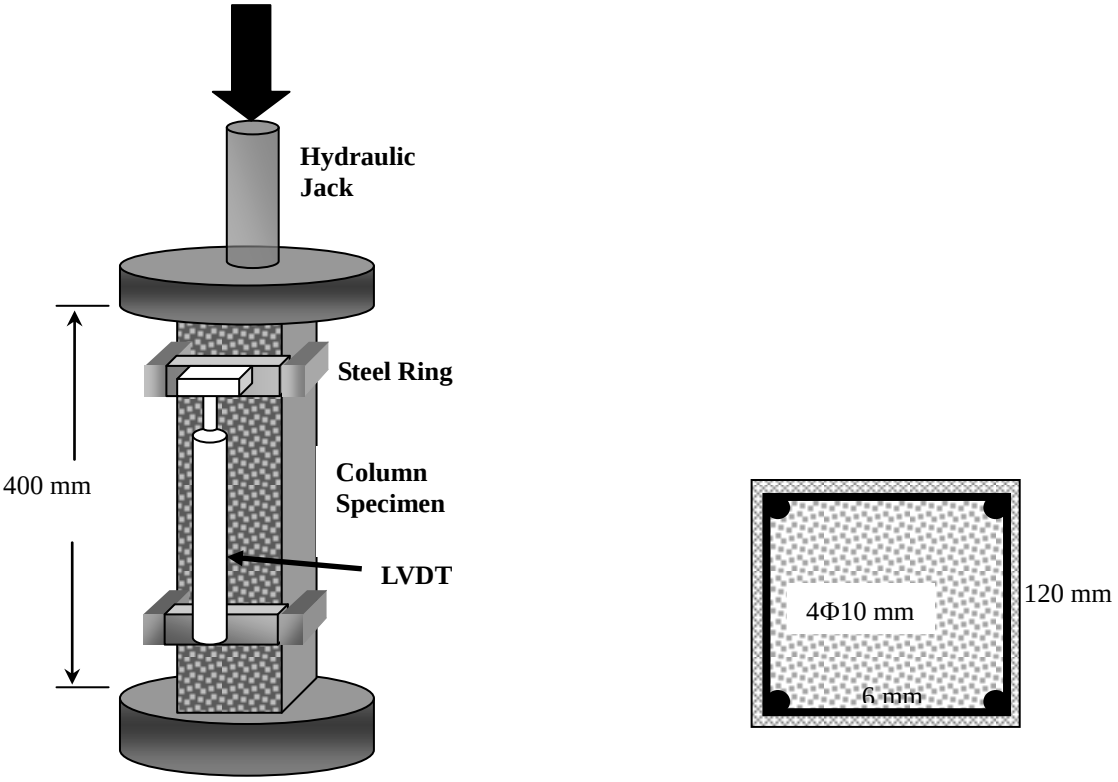

(a) Testing assembly (b) Cross section in column

Fig. 6 Schematic presentation of testing setup, specimen geometry and reinforcing steel detailing (dimensions in mm)

3.2 Validation of the proposed NLFE model

To validate the NLFE model, proposed in this paper, predictions for stress-strain diagram for thermally damaged RC columns and their characteristic (compressive stress capacity, axial stiffness and axial toughness) are compared to corresponding ones, experimentally determined by Haddad and Ashour (2013).

3.2.1 Stress-strain curve

The comparison between predicted and actual stress-strain diagram indicated excellent match for similar RC columns and exposure temperatures: Figs. 7-8 show selective stress-strain diagrams. As can be deduced, the predicted matched actual stress-strain diagrams and extended to higher strain values until failure showing a descending portion rather absent in actual ones. This suggests that predicted and actual mechanical properties (ultimate compressive strength, axial stiffness, and axial toughness) would be very close**.**

3.2.2 Compressive strength capacity of columns

The predicted compressive strength capacity (CSC) for the columns under investigation was depicted against actual ones, as shown in Fig. 9(a). As can be noticed, the slope of the line fitted

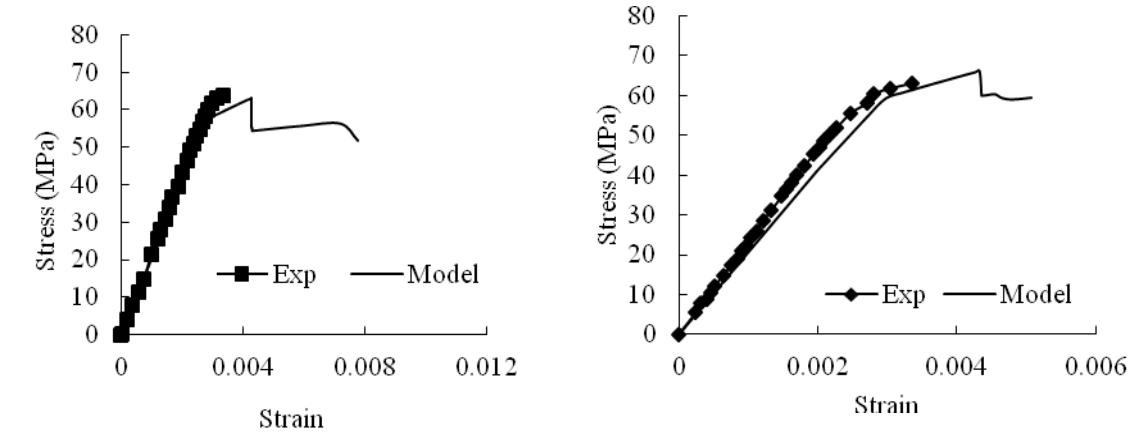

(a) No confinement

(b) No confinement

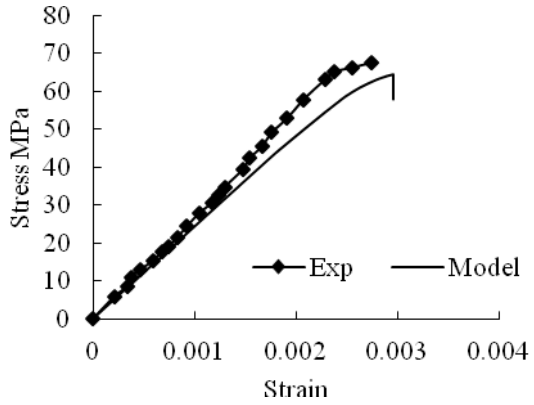

(c) Medium confinement

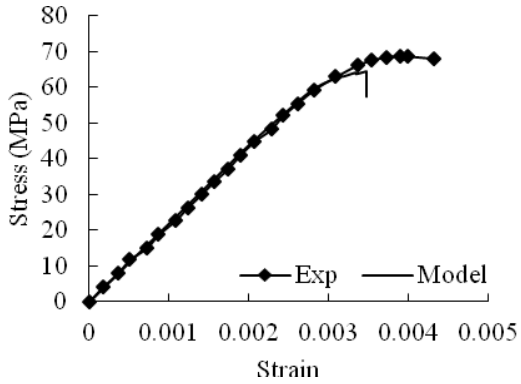

(d) Medium confinement

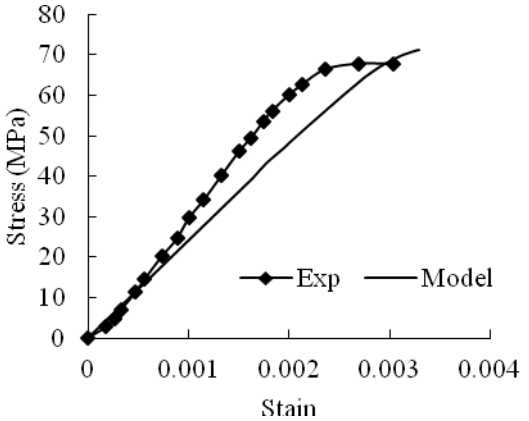

(e) Heavy confinement

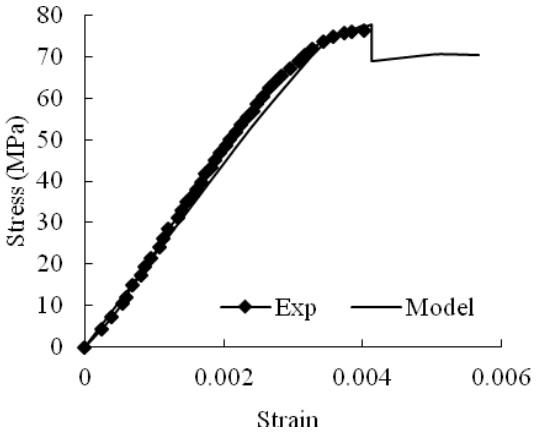

(f) Heavy confinement

Fig. 7 Stress-strain diagram for plain (left) and fibrous LWAC columns at three levels of steel ties confinements

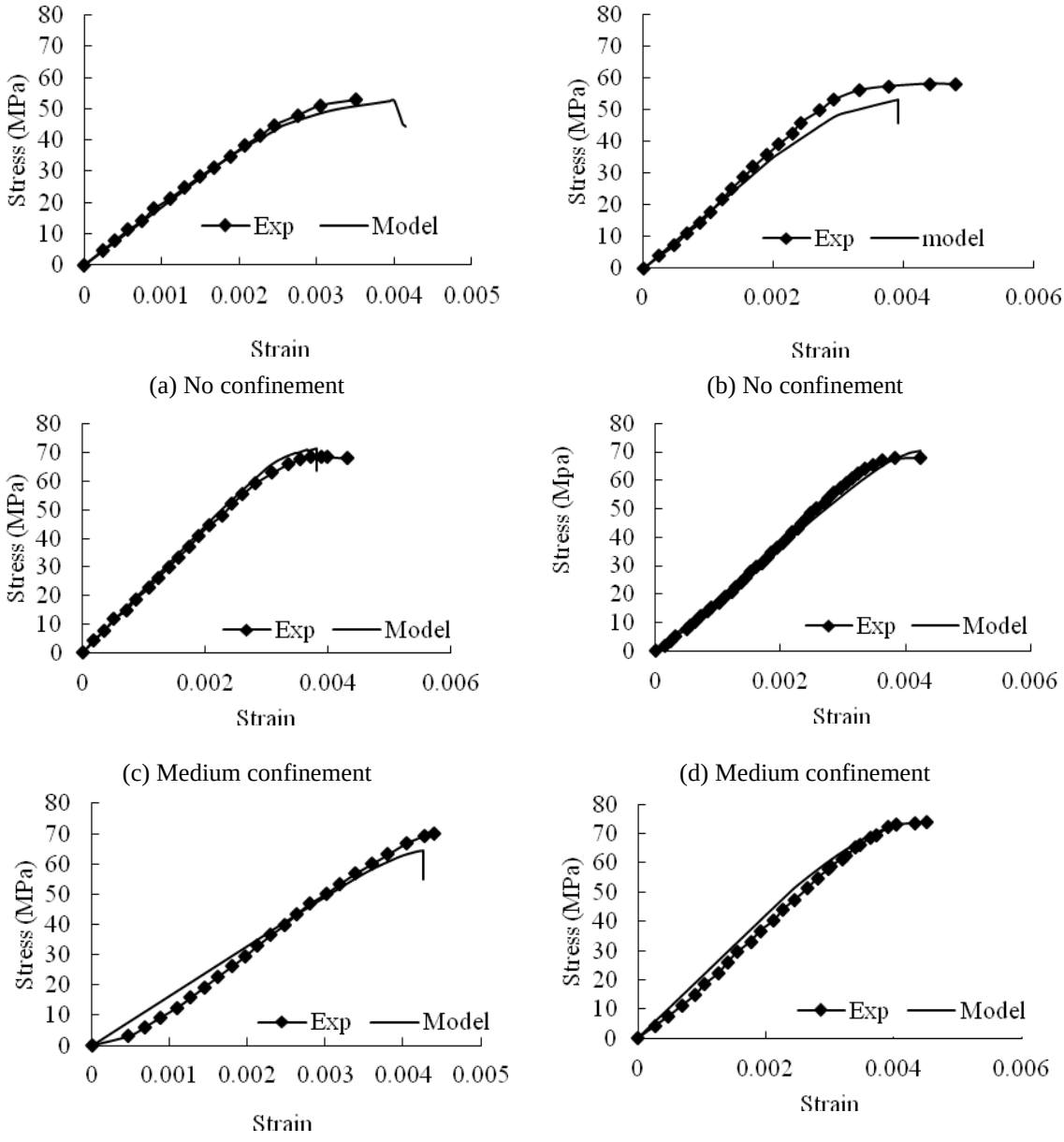

(a) No confinement (b) No confinement

(c) Medium confinement (d) Medium confinement

(e) Heavy confinement (f) Heavy confinement

Fig. 8 Stress-strain diagram for plain (left) and fibrous LWAC columns at three levels of steel ties confinements and subjected to 300℃

between predicted and actual CSC is very close to 45^{o} degrees; suggesting a very close match. The residual values, computed as the difference between predicted and actual divided by actual CSC, were plotted for different specimens; as shown in Fig. 9(b). The residuals show random distribution without a certain trend to indicate inappropriate model. The absolute error of prediction, which represented more than 90% of columns, was smaller than 10%.

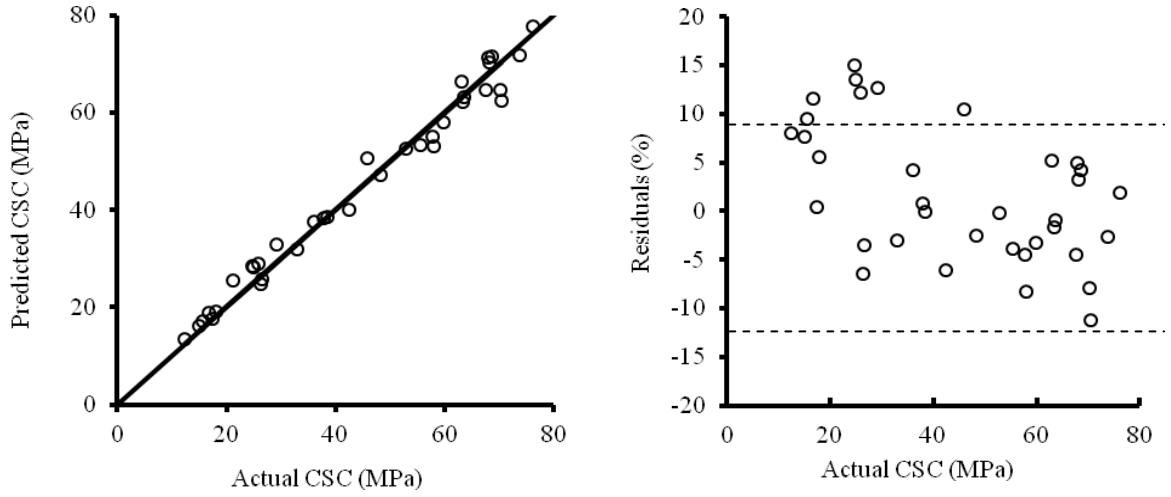

(a) Predicted versus actual CSC (b) Residual plot

Fig. 9 Statistical analysis of present model's predictability of CSC

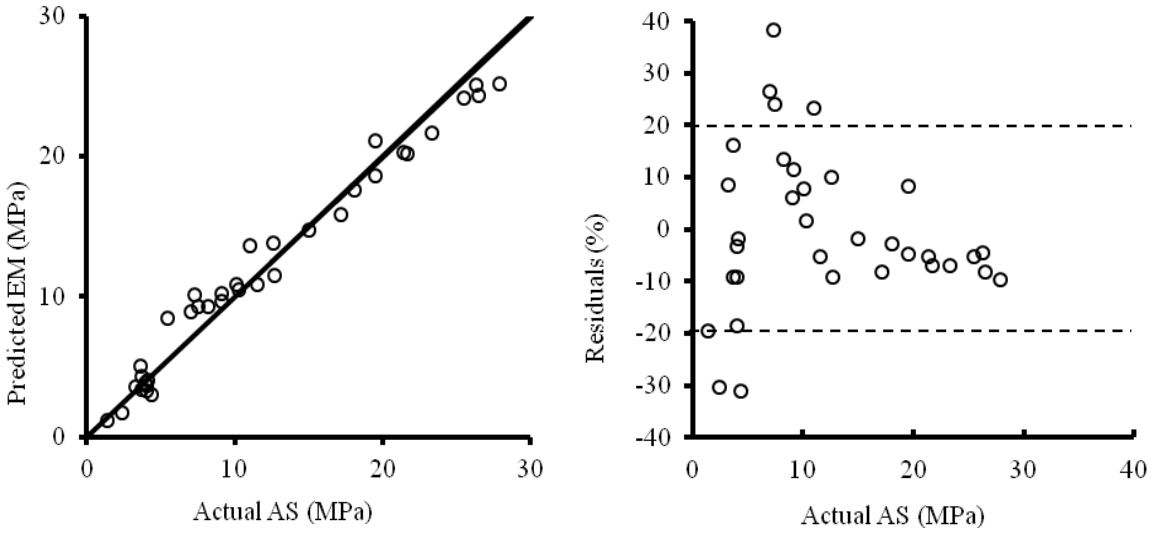

(a) Predicted versus actual AS (b) Residual plot

Fig. 10 Statistical analysis of present model's predictability of AS

3.2.3 Axial stiffness of columns

The predicted axial stiffness for the columns under investigation was depicted against actual ones, as shown in Fig. 10(a). The slope of the line fitted between predicted and actual axial stiffness is very close to 45° degrees; indicating a very close match. The residual values, computed as the difference between predicted and actual divided by actual stiffness, were plotted for different specimens; as shown in Fig. 10(b). The residuals show random distribution without a

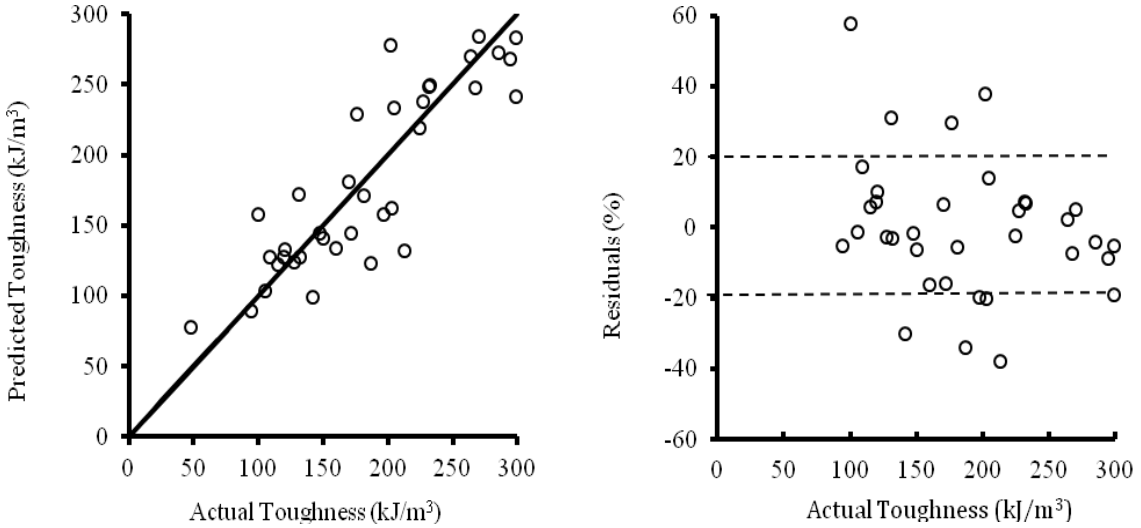

(a) Predicted versus actual toughness (b) Residual plot

Fig. 11 Statistical analysis of present model's predictability of toughness

certain trend to indicate impropriate model. The absolute error of prediction for more than 95% of columns was smaller than 20%.

3.2.4 Axial toughness of columns

The predicted versus actual axial toughness is depicted in Fig. 11(a) whereas corresponding residuals plot is depicted in Fig. 11(b). The toughness was calculated as the area underneath the stress-strain diagram up to ultimate stress so that comparison is made between predicted and actual values. The information provided by Fig. 11(b) showed that the matching between predicted and actual axial toughness is more than satisfactory.

Again, the residual plot indicates no specific trend to indicate that the present model is impropriate. The absolute error of prediction for more than 90% of columns was smaller than 20%.

Based on the above discussion, it can be stated that the NLFE model suggested had provided a very good level of prediction. Hence, it can be used with a significant level of confidence in further predictions that aid in understanding more the behavior of concrete and steel in post-heated columns, as presented in the following section.

3.3 Predictions using present NLFE model

Major characteristics for post-heating mechanical behavior of plain and fibrous columns has been obtained using the present model for selected temperature levels and four confinement levels by steel ties at spacing of (60, 30, 20, and 10 mm); corresponding to transverse steel ratios of (1.57, 3.14, 4.71, and 9.42%), respectively. Description and justification of trend behaviors of these characteristics versus exposure temperature and confinement level are presented in the following paragraphs.

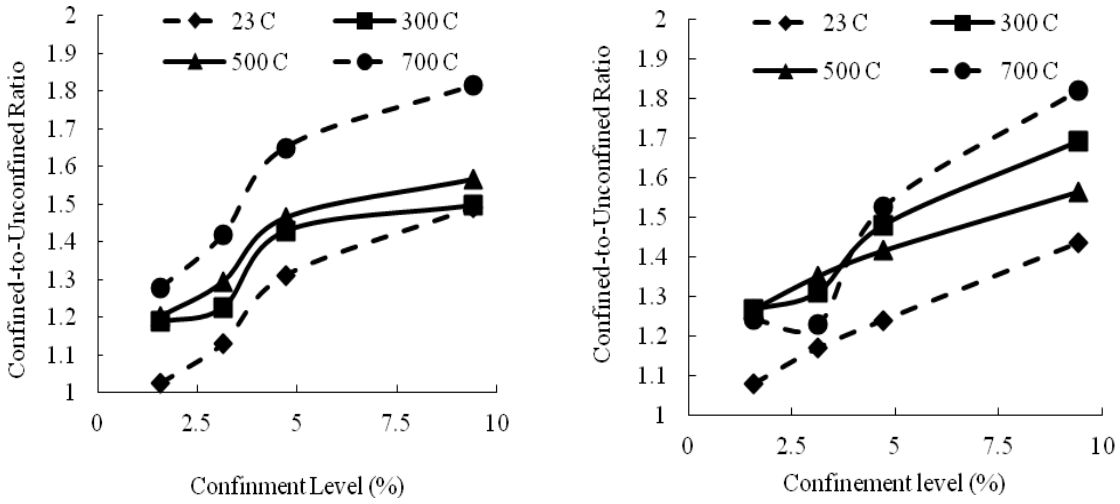

(a) without steel fiber (b) with steel fiber

Fig. 12 Ratio of confined to unconfined compressive load capacity (CSC) for post-heated LWAC columns

3.3.1 Compressive strength capacity of LWAC columns

Fig. 12 indicated a positive contribution of lateral reinforcement ratio on compressive strength capacity (CSC) for plain and fibrous LWAC columns. Compared to those without lateral reinforcement, plain LWAC columns, at 1.57 and 9.42% achieved an increase in their capacity of about (2.5, 20, 20, and 28%) and (50, 50, 57, and 81%) when pre-heated to (23, 300, 500 and 700℃), respectively. The curves showed a significant jump in CSC as lateral reinforcement ratio was raised to 4.71% with corresponding percentage increases of about (31, 43, 46, and 65%), respectively. Hence, the benefit of using higher lateral reinforcement in salvaging post-heating CSC for LWAC columns is more pronounced in preheated ones. On contrast, the percentage increase in CSC for fibrous LWAC columns, having lateral reinforcement ratio in the range from 1.57 to 9.42%, were slightly affected by exposure temperatures beyond 300℃, as can be concluded from Fig. 12(b). Furthermore, the use of heavy lateral reinforcement at 9.42% yielded noticeable improvement in CSC, proportional to temperature level. Slightly lower jump in CSC percentage increase was noticed for fibrous than plain LWAC columns when lateral reinforcement ratio was increased from 1.57 to 4.71%.

3.3.2 Axial stiffness for LWAC columns

In general, axial stiffness was significantly improved for post-heated plain and fibrous LWAC columns upon use of lateral reinforcement as can be deduced from Figs. 13. It is evident that the utmost increase in axial stiffness for plain LWAC columns was achieved for those pre-heated to 700℃ at 200% followed by those pre-heated to 500oC at 100%, Fig. 13(a). The lateral reinforcement ratio had a negligible effect upon the percentage increase in axial stiffness for exposure temperatures equal to or lower than 300℃. Except for those exposed to 700℃, other fibrous LWAC columns have demonstrated low sensitivity towards the increase in confinement level; owning to the significant contribution of fibers in mitigating heat and load-generated cracks, Fig. 13(b). The benefit of using lateral confinement in increasing axial stiffness was more pronounced for plain than fibrous LWAC columns.

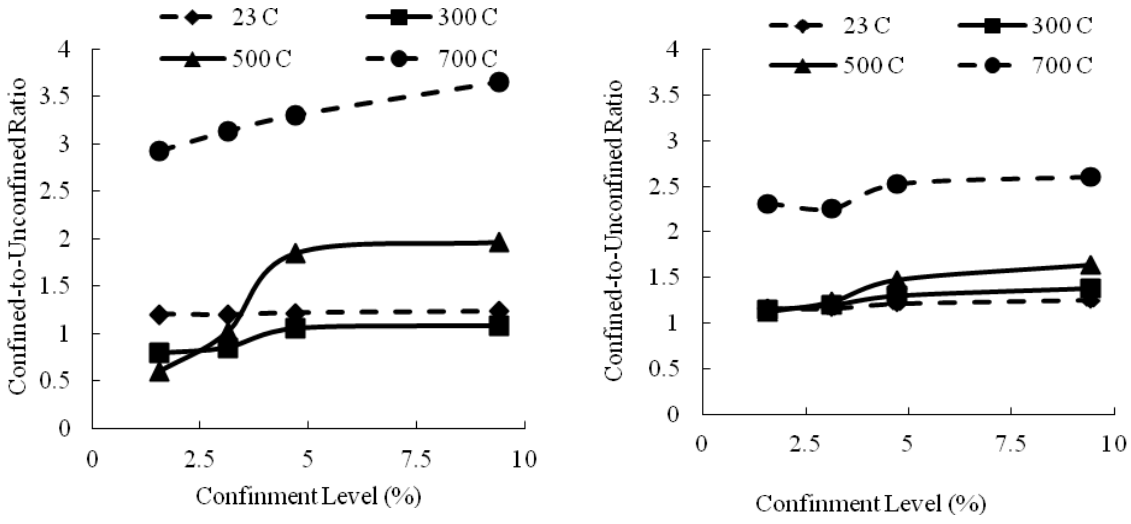

(a) without steel fiber (b) with steel fiber

Fig. 13 Ratio of confined to unconfined axial stiffness for post-heated LWAC columns

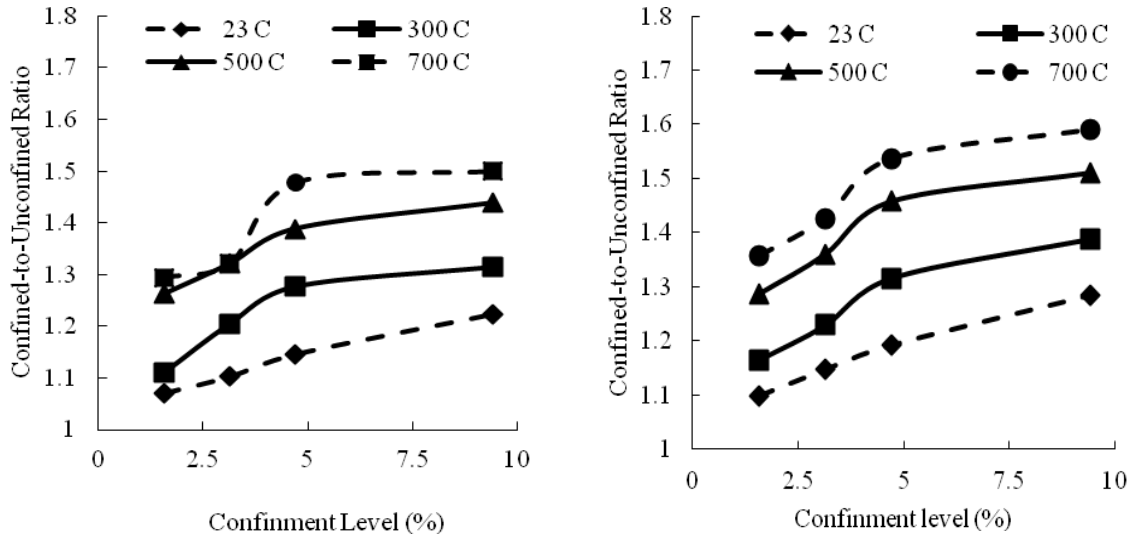

(a) without steel fiber (b) with steel fiber

Fig. 14 Ratio of confined to unconfined compressive strength of concrete for LWAC of post-heat RC columns

3.3.3 Compressive strength of concrete

The confined strength for intact concrete is increased with ties reinforcement ratio traditionally computed upon a well-stipulated empirical formula, ACI 318-011 and Mander *et al.* (1988). Such a formula cannot be applicable for post-heated and confined LWAC; as noticed from the data of Fig. 14: the ratio of confined to unconfined compressive strength for plain and fibrous LWAC in RC columns is dependent upon lateral reinforcement ratio as well as exposure temperature. The

findings indicated clearly that contribution of confinement by steel ties to promoting the confined compressive strength of plain and fibrous LWAC in RC columns is proportional to exposures temperature level. The highest percentage increases in compressive strength upon confinement with 9.42% lateral steel ratio were (22, 32, 44, and 50%) for plain LWAC and (28, 39, 52, and 59%) for fibrous LWAC; suggesting that the benefit of using ties confinement is reflected more in fibrous rather plain LWAC.

4. Conclusions

A NLFE model was developed in this work to predict post-heating mechanical behavior of columns, cast with plain and fibrous LWAC, using ANSYS software. The model was validated using experimental published results before its prediction were extended to understand more the behavior of these columns. Based on the results and findings, the following conclusion can be stated:

1. The NLFE method considered the degradation in mechanical properties of LWAC and steel with temperature and relied on the empirical formulae by European code in obtaining mechanical parameters necessary for the model's computations.
2. The NLFE method predictions of post-heating mechanical behavior of columns, as represented by stress-strain diagram and its characteristics, matched very well with corresponding experimental results.
3. The NLFEM model predictions were extended to study the effect of steel confinement on post-heating mechanical behavior of LWAC columns. The results revealed the importance of lateral steel confinement in salvaging the mechanical behavior of LWAC columns subjected to elevated temperatures.
4. The predictions by the present NLFEM model shall be very helpful in providing additional data to adjust the formulation of available empirical models, used to predict confined compressive strength of post-heated LWAC, and hence improve their predictability.

References

ACI Comitte 318 (2011), Building Code Requirements for Structural Concrete and Commentary (ACI 318-011), American Concrete Institute Detroit, MI.

Ahmed, A.H. and Hasan, H.M.A. (2005), "Effect of cyclic heating on reinforced concrete thick slabs", *Al-Rafidain Eng. J.*, **4**(13), 35-51.

ANSYS (2008), User's manual Version 11.0.

Al-Nimry, H, Haddad, R., Afram, S., Abdel-Halim, M., Haddad, R.H. and Ashour, D.M. (2013), "Effectiveness of advanced composites in repair heat-damaged RC columns", *Mater. Struct.*, **46**, 1843-1860.

Banthia, N. and Sappakittipakorn, M. (2007), "Toughness enhancement in steel fiber reinforced concrete through fiber hybridization", *Cement Concrete Res.*, **37**, 1366-1372.

Chen, B. and Liu, J. (2005), "Contribution of hybrid fibers on the properties of the high-strength lightweight concrete having good workability", *Cement Concrete Res.*, **35**(5), 913-917.

Demirbog, R. and Gu, R. (2003), "The effects of expanded perlite aggregate, silica fume and fly ash on the thermal conductivity of lightweight concrete", *Cement Concrete Res.*, **33**, 723-727.

Dwaikat, M.B. and Kodur, V.K.R. (2009), "Hydrothermal Model for Predicting Fire Induced Spalling in

Concrete Structural Systems", *Fire Saf. J.*, **44**, 425-434.
Eurocode 4 (2005), Design of composite steel and concrete structures-Part 1-2: General rules-structure fire design, EN 1994-1-2, Final draft, European Committee for Standardization.
Haddad, R. and Ashour, D. (2013), "Thermal performance of steel fibrous lightweight aggregate concrete short columns", *J. Compos. Mater.*, **47**(16), 2013-2025.
Haddad, R.H., Shannag, M.J. and Moh'd, A. (2008), "Repair of heat-damaged RC shallow beams using advanced composites", *Mater. Struct.*, **41**(2), 287-29.
Hossain, K.M.A. (2006), "Blended cement and lightweight concrete using scoria: mix design, strength, durability and heat Insulation characteristics", *Phys. Sci.*, **1**, 5-16.
Huang, Z.H. (2010), "Modelling the bond between concrete and reinforcing steel in a fire", *Eng. Struct.*, **32**(11), 3660-69.
Hu, H.T. and Schnobrich, W.C. (1989), "Constitutive modeling of concrete by using nonassociated plasticity", *J. Mater. Civil Eng.*, ASCE, **1**(4), 199-216.
International Organization for the Development of Structural Concrete (FIP) (1983), FIP Manual of Lightweight Aggregate Concrete, John Wiley and Sons, Toronto, NY.
Issa, M.S. and Anwar, H. (2004), "Structural behavior of high strength reinforced concrete columns exposed to direct fire", *Proceeding of International Conference on Future Vision and Challenges for Urban Development*, Egypt..
Kayali, O. (2008), "Fly ash lightweight aggregates in high performance concrete", *Constr. Build. Mater.*, **22**, 2293-2299.
Lawson, J.R., Phan, L.T. and Davis, F. (2000), "Mechanical properties of high performance concrete after exposure to elevated temperatures", Report, National Institute and Standards and Technology, IR 6475, National Technical Information Service (NTIS), Technology Administration, U.S. Department of Commerce, Springfield, VA.
Mander, J.B., Priestley, M.J.N. and Park, R. (1988), "Theoretical stress-strain model for confined concrete", *Struct. Eng. J.*, ASCE, **114**(8), 1804-26.
Mouli, M. and Khelafi, H. (2008), "Performance characteristics of lightweight aggregates concrete containing natural pozzolan", *Build. Environ.*, **43**, 31-36.
Nizamuddin, Z. and Bresler, B. (1979), "Fire resistance of reinforced concrete slabs", *J. Struct. Div.*, **8**(105), 1653-1671.
Omer, A. (2007), "Effects of elevated temperatures on properties of concrete", *Fire Saf. J.*, **42**, 516-522.
Pothisiri, T. and Panedpojaman, P. (2012), "Modeling of bonding between steel rebar and concrete at elevated temperatures", *Constr. Build. Mater.*, **27**(1), 130-140.
Seanz, L. (1964), "Discussion equation for the stress stain curve of concrete, By Desayi P, Krishnan S", *ACI J.*, **61**(3), 1229-1235.

CC